CMOS Device Modeling for Subthreshold Circuits

Michael D. Godfrey

Information Systems Laboratory
Electrical Engineering Department
Stanford University

1. Introduction

The increasing use of standard CMOS processes for construction of circuits which operate in the subthreshold (weak inversion) regime leads to the need for a reliable model of device behavior in this regime. The model should be reasonably accurate with respect to device scale for present and future technologies and with respect to a reasonable range of values of technology parameters. The form of the model should lend itself to efficient computation and should fit into suitable circuit models. Ideally, the model should cover above threshold operation, but it is essential that it yield accurate results in the transition between the two regimes. More precisely, the results should be accurate for the circuit variables which significantly affect the behavior of typical constructions. For example, it should be possible to accurately compute gain and conductance. Tsividis [6] has pointed out that obtaining such accuracy is not as straightforward as might be thought, even when IV curves appear to be highly accurate.

It would be particularly useful if the model had broad *predictive* power, i.e. it would normally get fairly accurate results, given measured parameters from the processing run (not necessarily the wafer or chip or device), without the need for "adjustments" of "uncontrolled" parameters.

There has been a substantial amount of modeling work which has addressed behavior in subthreshold (cf. [3, 4, 5, 6, 8, and 9]). This work provides a wealth of background and useful analysis. The work reported by C.C. Enz, in his Ph.D. thesis [1], has the additional feature that it seems to provide an efficient computational form that covers subthreshold, inversion, and the transition between regimes. It does not provide a model of operation in the linear regime.

This paper reports on experience in using this model, and work that has been carried out to develop the model so that it yields accurate results for, for example, present MOSIS-provided processes. The main effort in doing this was to develop the model so that it is based on device parameters that are valid in the subthreshold regime. Previous work has tended to use measurements done in strong inversion and extrapolate them to subthreshold, and to force a correspondence between approximations above and below threshold. A result of this approach has been that the model works well for the square-law regime, but shows large errors when used in subthreshold. The key parameters that require careful treatment are the threshold voltage,

V_t, and the pre-exponential constant, I_0. V_t is famous for its many conflicting definitions [6]. I_0 is well-known as the place where all the "left-overs" are dumped. In order to expect reasonable predictive power, both of these parameters need precise, measurement-based, definitions.

2. Classical Derivations

The classical model equations are:

$$I_{ds} = \begin{cases} S\beta\left[(V_{gs}-V_t)V_{ds} - \dfrac{V_{ds}^2}{2}\right] & 0 < V_{ds} < V_{gs}-V_t;\ \text{linear} \\ \dfrac{S\beta}{2}\left[\left(V_{gs}-V_t\right)^2(1+\lambda V_{ds})\right] & 0 < V_{gs}-V_t < V_{ds};\ \text{strong inversion} \end{cases}$$

where I_{ds} is the drain-source current, S = channel width to length ratio (W/L), $\beta = \mu C_{ox}$ where μ is the carrier mobility, $C_{ox} = \epsilon/t_{ox}$ where ϵ is the permitivity of the gate insulator and t_{ox} is the thickness of the gate insulator, V_{gs} is the gate-source voltage, V_{ds} is the drain-source voltage, V_t is the threshold voltage, and λ is the linear channel length modulation (Early) factor.

The corresponding, simplified, result for the subthreshold saturation regime is:

$$I_{ds} = I_0\left(\frac{kT}{q}\right)^2 e^{-\frac{q\kappa V_g}{kT}}\left(e^{\frac{qV_s}{kT}} - e^{\frac{qV_d}{kT}}\right) + g_d V_{ds}$$

where I_0 is the pre-eponential constant (to be discussed below), V_g is the gate voltage, V_s is source voltage, V_d is drain voltage all relative to substrate, κ is the body effect ($\kappa = \frac{\partial\psi_s}{\partial V_g}$, where ψ_s is the surface potential), k is Boltzmann's constant, T is temperature, q is the charge on an electron, and $g_d = \frac{\partial I}{\partial V_d}$ is the coefficient for channel length modulation (Early) effect. Note that the effects of channel length modulation appear to be different between above and below threshold. Therefore, there is likely not a simple relationship between λ and g_d.

The problem now is to try to match up the strong inversion (square law) expression and that for subthreshold. This looks easier than it is. However, note that if, in the square law expression, $(V_{gs} - V_t)$ is divided by $kT/2q$ (the justification for the factor 2 will be explained below) then the "constant" terms:

$$I_{0,sq} = S2\beta\left(\frac{kT}{q}\right)^2 \qquad \text{square-law}$$

and

$$I_{0,sb} = SI_0\left(\frac{kT}{q}\right)^2 \qquad \text{subthreshold}$$

at least have the same dimensions of current. A preview of the problem of near-threshold operation is that I_0 is not likely to be equal to 2β since its dependence on the gate-channel capacitance may be different from that of β.

Another problem is that the simplifying assumptions, typically linearization about some operating point by first-order Taylor Series approximation, in both above and subthreshold may not be sufficiently accurate approximations to be useful in the transition region. In addition, the role of V_t has added considerable confusion and is critical to accurate results. It is important to note that V_t is not a physical constant, but rather it is a point value which is intended to distinguish between two regimes which have no discontinuous boundary. Unfortunately, a number of theoretical and empirical definitions of V_t are in use, and they produce wildly differing results. The usual definition is that V_t is the gate voltage such that the current due to drift is equal to the current due to diffusion. However, this is not a state that is directly measurable and therefore various indirect methods are used for measurement. Tsividis [6] makes this problem abundantly clear and shows specific examples of the resulting errors. The consequences of this problem for the Enz-Vittoz-Oguey model are discussed below.

3. The Problems of the Transition Region

The basic problem of the transition region is that there is no clear understanding of the interaction of the potentials in the channel in the situation where part of the current is due to drift and part due to diffusion. The relationship between V_p, pinchoff voltage, and V_t is unclear in this region. There is a tendency to use V_p and V_t interchangeably in much of the literature. Specifically, equations similar to those above given above, but as a function of V_p instead of V_t, are sometimes used. This is the case in the Enz-Vittoz-Oguey derivation below.

One approximation for V_p is $V_p = \kappa(V_g - V_t)$. If the subthreshold equation is written using V_p in place of V_t, and this approximation for V_p is substituted then a term of the form e^{V_t} appears in the preexponential I_0 term. The dependence of the preexponential term on V_t can have a very large effect on device behavior and on any understanding of the sources of variation in currents and in conductance. However, the standard subthreshold model does not give rise to a V_t term in the preexponential constant.

The transition region is larger than one might guess. The strong inversion model predicts zero current for any gate voltage below V_t, with the current dropping to zero as the square of the gate-threshold voltage difference. The subthreshold model predicts a log-linear current for any gate voltage. The slope of the IV curve will start to diverge from log-linear well before the threshold voltage. Thus, there is a region of width on the order of 0.5 volt in which neither model provides anywhere near correct behavior. Since the error first appears as a change in the slope of the IV curves, it greatly affects all behavior that depends on the derivative of current with respect to voltage.

4. The Enz/Vittoz Model

The model described by Enz is based on prior work by Vittoz and Oguey, and was developed under Vittoz's supervision. A key mathematical approximation used in the model is due to Oguey (see below). Therefore, we will refer to the model as the Enz/Vittoz/Oguey (EVO) Model. In the following Sections we develop the model from device equations, following the derivations in Enz, but also pointing out some additional consequences of the derivation and approximations.

In is essential to keep in mind that, for our purposes, the model should behave well for devices in subthreshold. Thus, gate voltages are intended to be well below threshold voltage and typical I_{ds} values are around or below $10^{-9}A$.

4.1 Weak Inversion

The equation for drain current in weak inversion used by Enz in [1] takes the form:

$$I_d = K_W S \beta U_T^2 \left(e^{\frac{(V_p - V_s)}{U_T}} - e^{\frac{(V_p - V_d)}{U_T}} \right) \tag{1}$$

where:

variable	definition	demensions
S	= channel width/length ratio (W/L)	dimensionless
U_T	$= \frac{kT}{q} = V_k = 0.025v$ at room temperature	V
I_d	drain current	μA
β	$= \mu C_{ox} \approx 50 \mu A/V^2$	$\mu A/V^2$
K_W	Adjustment factor	dimensionless
n	$= 1/\kappa \approx 1.4$ Charge effect due to substrate	dimensionless
V_{T0}	Threshold voltage (ref. substrate)	V
V_p	$= \frac{1}{n}(V_g - V_{T0})$ Pinchoff voltage	V
V_s	Source voltage (ref. substrate)	V
V_d	Drain voltage(ref. substrate)	V

4.2 Strong Inversion

In strong inversion current flow is governed by *drift.* In order to match the functional form required for the approximation (explained below) Enz derives the following square law equation:

$$I_d = \frac{nS\beta}{2}((V_p - V_s)^2 - (V_p - V_d)^2). \tag{2}$$

However, he points out, but does not comment on, the fact that this equation is valid only in the conduction regime defined by:

$$V_s \text{ and } V_d < V_p.$$

In order to make this equation more nearly consistent with standard derivations $V_p - V_s$ and $V_p - V_d$ should be replaced by $\max(V_p - V_s, 0)$ and $\max(V_p - V_d, 0)$. This change does not conflict with the subsequent use of the equation in the EVO model, and yields conventional square-law behavior in the above-threshold regime. However, this is not a valid model in the region near subthreshold where gate voltages are relatively low, and therefore either V_s or V_d will approach V_p. With this modification, the expression is:

$$I_d = \frac{nS\beta}{2}(max(V_p - V_s, 0))^2 - max(V_p - V_d, 0)^2). \tag{3}$$

This expression covers conduction and strong inversion with both forward and reverse saturation. This leaves the problem of finding an approximation that connects the regions of strong and weak inversion.

4.3 The Enz/Oguey Approximation

The key result in Enz's thesis is an approximation* which covers both weak and strong inversion without discontinuity. The approximation is based on the function $F(x)$ such that:

$$F(x) = \begin{cases} (\frac{x}{2})^2 & x >> 0 \\ e^x & x << 0. \end{cases} \tag{4}$$

The function that approximates this behavior is:

$$F(x) = \ln^2(1 + e^{x/2}). \tag{5}$$

It can be seen that this function behaves like equation (4) by considering the two cases, $x >> 0$ and $x << 0$. For $x >> 0$,

$$F(x) \approx \ln^2(e^{x/2}) = (x/2)^2.$$

For the case $x << 0$, note that if $\epsilon << 0$, $e^\epsilon \approx 1 + \epsilon$. Therefore, $\ln(1 + \epsilon) \approx \epsilon$ and,

$$F(x) = e^x.$$

Now, if the strong inversion equation (3) is rewritten as

$$I_d = 2nS\beta U_T^2\left(\left(\frac{max(V_p - V_s, 0)}{2U_T}\right)^2 - \left(\frac{max(V_p - V_d, 0)}{2U_T}\right)^2\right)$$

* The references for the original suggestion of this approximation given in the thesis are:

[1] H.J. Oguey and S. Cserveny, “MOS Modelling at low current density,” *Summer Course on Process and Device Modelling,* ESAT Leuven-Heverlee, Belgium, June 1983.

[2] H. Oguey et S. Cserveny, “Modèle du transistor MOS valable dans un grand domaine de courants,” Bull. SEV/VSE, Feb. 1982.

and K_W is set equal to $2n$, comparing the weak and strong inversion equations shows that

$$I_d \propto F\left(\frac{V_p - V_s}{U_T}\right) - F\left(\frac{V_p - V_d}{U_T}\right) \tag{6}$$

where:

$$F(x) = \ln^2(1 + e^{\frac{x}{2}}).$$

It is the assignment of $K_W = 2n$ that forces the pre-exponential constant in both regimes to have the value derived from the strong inversion model. Figure 1 shows the following three functions:

$$\begin{aligned} F_1(V_g) &= \ln^2\left(1 + e^{(V_p - V_s)/(2U_T)}\right) - \ln^2\left(1 + e^{(V_p - V_d)/(2U_T)}\right) \\ F_2(V_g) &= \left(max(V_p - V_s, 0)\right)^2 - \left(max(V_p - V_d, 0)\right)^2 \\ F_3(V_g) &= e^{(V_p - V_s)/U_T} - e^{(V_p - V_d)/U_T} \end{aligned} \tag{7}$$

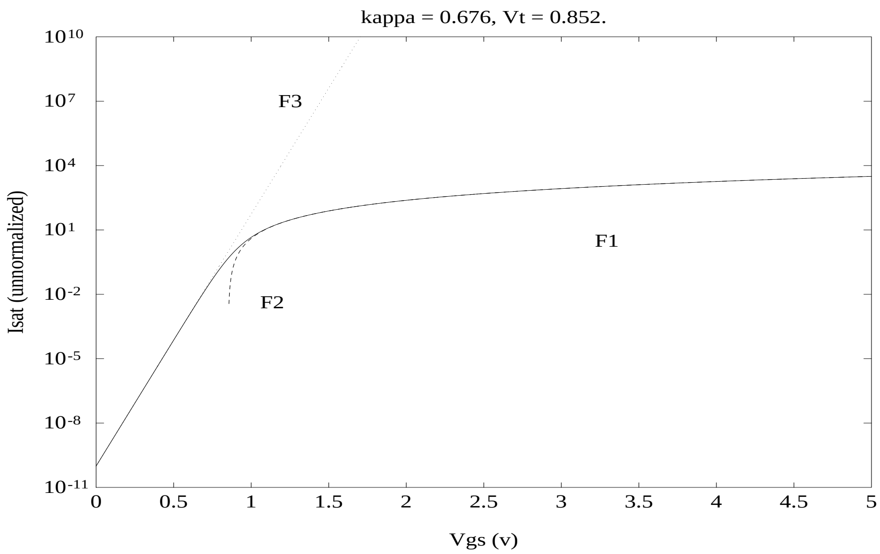

Figure 1: Behavior of Approximation

However, these equations require that $2\beta = \beta/\kappa$ or that some additional parameter be introduced into either the above or below threshold equations. Enz [1] introduced a factor K_W for this purpose. The justification for this is not clear.

4.4 The Enz/Oguey Approximation in Computational Form

One of the very nice features of the Enz/Oguey approximation is its computational simplicity. Using the approximation $V_p = \kappa(V_g - V_t)$ we can write equations (7) as*:

$$\begin{aligned} K_1 &= 2nS\beta U_t^2/\kappa \\ I_f &= \ln^2\Big(1 + exp\frac{\kappa(V_g - V_t) - V_s}{2U_t}\Big) \\ I_r &= \ln^2\Big(1 + exp\frac{\kappa(V_g - V_t) - V_d}{2U_t}\Big) \\ I_{ds} &= K_1(I_f - I_r)(1 + \lambda V_d) \end{aligned} \qquad (8)$$

where λ is the slope term from the linearized Early effect in the square-law regime (See Section 6.2).

However, note that this form has carried over the constant term, $2nS\beta U_t^2/\kappa$, from the strong inversion regime. This may lead to large errors if the equations are used for subthreshold. For $V_g < V_t$ equation 8 takes the form:

$$\begin{aligned} I_{ds} &= K_1\left(e^{\frac{(\kappa(V_g - V_t) - V_s)}{2U_t}} - e^{\frac{(\kappa(V_g - V_t) - V_d)}{2U_t}}\right) \\ &= K_1 e^{\frac{\kappa(V_g - V_t)}{U_T}}(e^{\frac{V_s}{U_t}} - e^{\frac{V_d}{U_t}}) \end{aligned}$$

The occurrence of V_t in the exponent of the "pre-exponential constant" is the source of the claim that lack of process-control of V_t leads to instability of I_{ds} for subthreshold devices.

5. Experimental Results

With the model in this form, and available in MatLab, it is a simple matter to use it to investigate reported or measured data from transistors operated in subthreshold. Equations (8), written in MatLab, are shown in the Appendix.

5.1 Results reported by Enz

Enz's Thesis contains plots of experimental measurements with the model curves fitted to the data points. His procedure was to adjust the model parameter values to get the "best" fit. This shows that the model has a suitable functional form, and sufficient parameters, so that it can be made to fit experimental data very closely. It does not however indicate whether the model can be used to predict results given *measured* values of the parameters.

5.2 Anomalies in Subthreshold Behavior

The study of device models for subthreshold behavior presents a number of anomalies which need to be explained before much confidence can be established in the correctness or predictive power of the models. Here are a few such anomalies.

* This is the form implemented by John Lazzaro in the analog simulator, anaLOG.

5.2.1 Failure to Predict I_d and I_{sat}

An example of IV curves for subthreshold devices is shown in [3], Figures 3.6 and 3.7. The device and process parameters for the measured devices are given in the text. The following figures show the same plots (of I_d vs. V_{ds} and I_{sat} vs. V_{gs}) as in Figures 3.6 and 3.7 in [3]. In Figure 3 we adjusted the process parameters and an additional scale parameter to produce a close approximation to the Figures in [3]. In order to get an approximate fit it was necessary to use a scaling factor (I_f) of 80. Figure 4 shows the result of using the measured process parameter values directly and setting the scaling factor to 1.0. Comparing Figure 4 with either Figure 3 or the Figures from [3] shows a difference in current values of a factor of about 80.

Discrepancies of this magnitude can have harmful effects on analog designs.

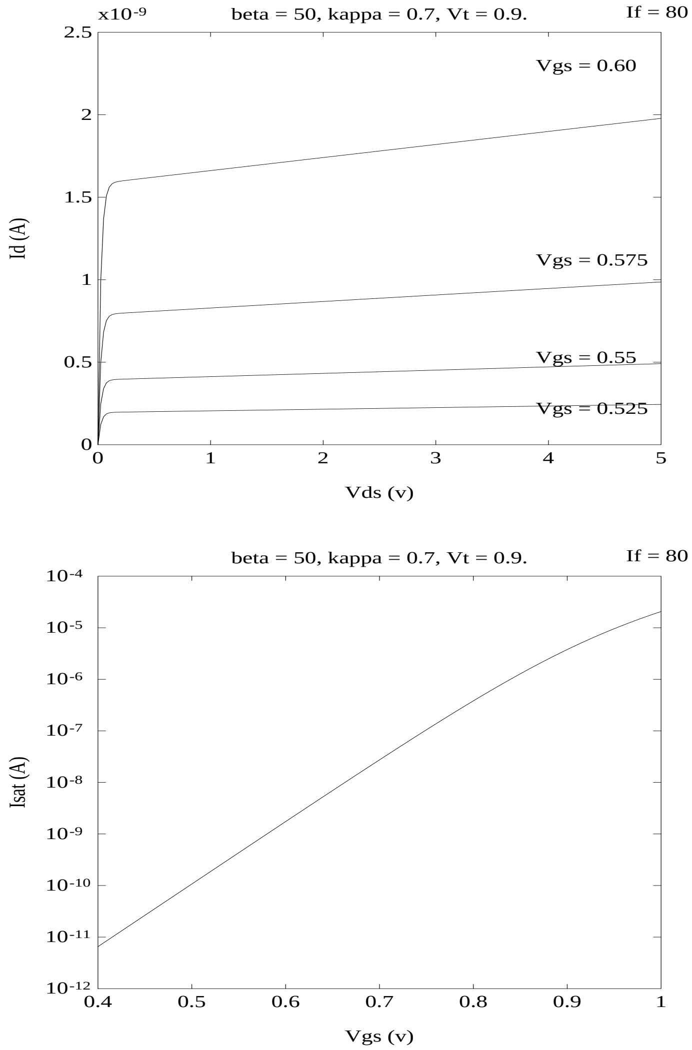

Figure 3: Approximate Reproduction of Figures 3.6 and 3.7 of [3]

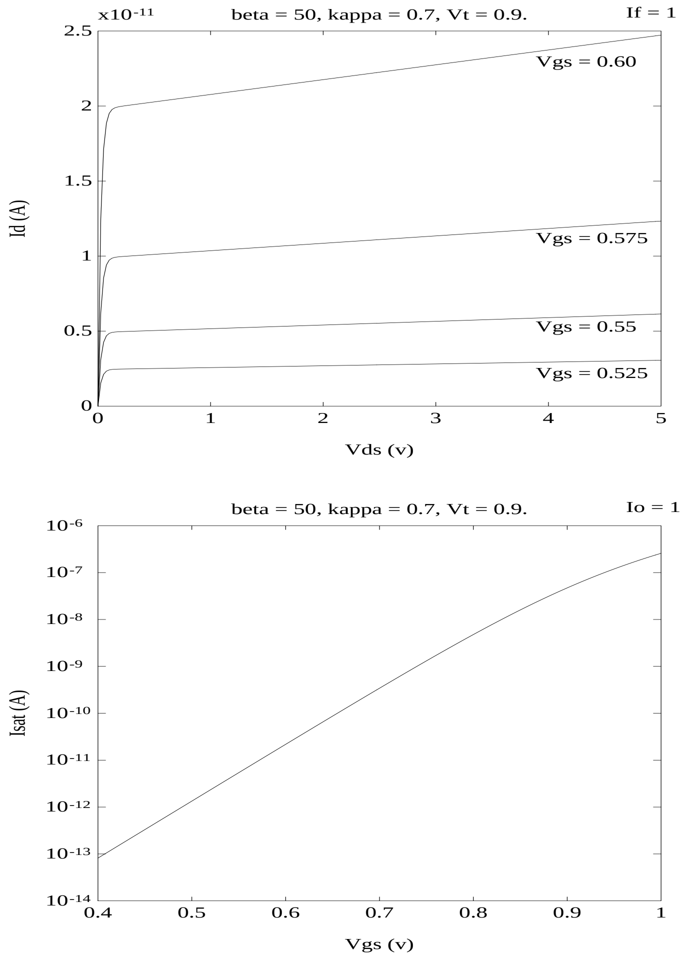

Figure 4: Enz/Vittoz Model Using Device Parameters from [3]

5.2.2 Magnitude of the Early Effect

It appears from data published in [3] (Figure B.3, pg. 325) that the Early Effect may be approximated as a linear function of channel length. If a linear equation is roughly fitted using the data from Figure 3 one gets:

$$V_0 = -6.9 + 17.3L. \tag{9}$$

However, use of this equation in the EVO model produces I_d curves whose slope is about 3 times those shown in Figure 3.7 in [3]. This discrepancy is shown in Figure 5.

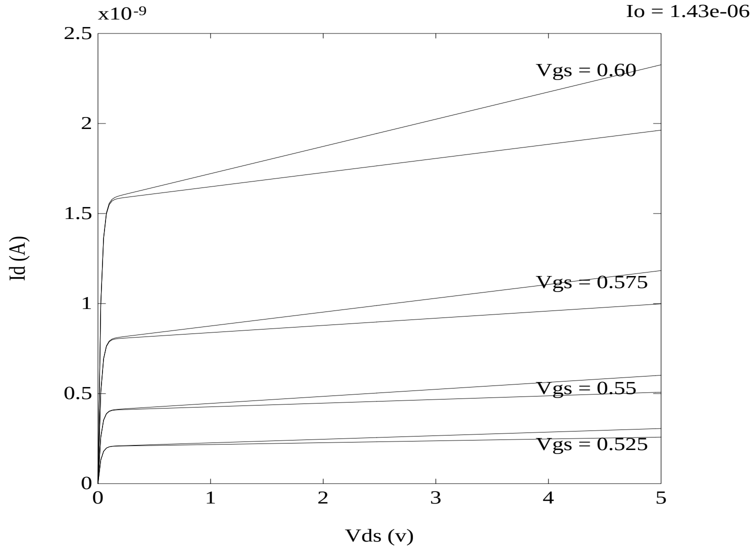

Figure 5: Incorrect Slope of Linear Early Effect

6. Improvement to the Model

The mathematical attractions of the EVO model provide an incentive to find the source of the problems with its use for accurate description and prediction. Investigation shows that a major source of problems is the definition and measurement of V_{th}, and relation of V_{th} to I_0 and κ.

6.1 Measurement of V_{th}

The standard method of measuring V_{th} is:

1. Set V_{ds} to some value which is much less than twice the Fermi potential, such as $0.05v$.

2. Measure I_d vs. V_g for values of V_g from 0 to about $2v$.

3. Extrapolate the linear part of the resulting curve (above V_{th}) back to the I_d origin. This value of V_g is the measured V_{th}.

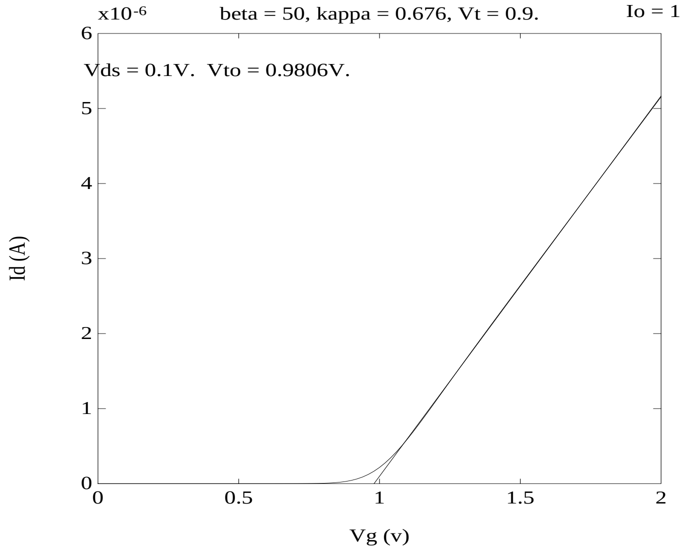

Figure 6: "Measurement" of V_{th} from EVO Model

If this measurement procedure is applied to the EVO model (pretending the model is a transistor) a result like that shown in Figure 6 is obtained. In the Figure, V_t is the threshold voltage used by the model and V_{t0} is the threshold voltage value measured from the model output. This shows immediately that the threshold voltage used by the model and the measured value are substantially different. The magnitude of the difference depends on the value of V_{th} and on the value of V_{ds} used in the measurement. However, this measurement procedure for V_{th} measures device performance in the linear regime. The EVO model is not valid in this regime.

7. Sensitivity of I_{ds} to V_{th}

It is often stated (for example in [2]) that the source of variation in I_{ds} is lack of process control over V_{th}. As has been shown above, part of the problem stems from inconsistent definitions of V_{th}. However, it is also clear that variation in V_{th} can be a source of unexpected variation in I_{ds}. Because of the exponential dependence of I_{ds} on V_{th}. Very small variation in V_{th} produces a large variation in I_{ds}. Figure 9 shows this effect.

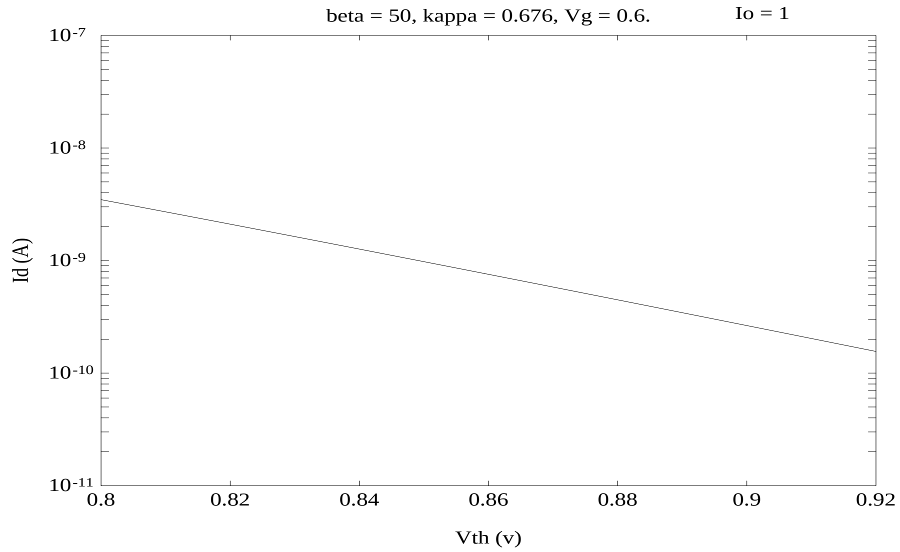

Figure 9: Dependence of I_{ds} on V_{th}.

A one percent change in V_{th} yields a nearly 20 percent change in I_{ds}. It is unrealistic to expect control of V_{th} below about a percent, but this it what would be required if values of I_{ds} with accuracy better than 20% were to be obtained. Pavasović, Andreou and Westgate [7] and Pavasović [8] have investigated variation in drain current in subthreshold within individual die. The results that they report are from modern standard fabrication processes, such as those provided through MOSIS. They constructed arrays of transistors so that they could measure variation in behavior as a function of position on the die. An important conclusion in their work is that the spatial variation (which also, curiously, has a distinct spatial periodicity) was, in terms of measured current, about 2% for 16 by 16μm transistors and about 7.2% for 4 by 4μm devices. This variation, if it is really due to variation in V_{th}, represents less than 0.5% variation in V_{th}. Some fabricators have recently claimed to be able to hold V_{th} to within 1%. These results and claims suggest that the minimum device to device variation in I_{ds} that is likely to be achievable will be above 20%. This, however, is a variation which is comparable to other device variation. It is much less than seems to have been suggested in previous literature.

7.1 Measurement of I_0, κ, and V_{th}

The most direct way to achieve good results in the subthreshold regime, using this model, is to directly measure I_0 for the process being used. It may, in addition, prove to be possible to develop an accurate model of I_0 as a function of physical and process parameters. We have made a number of measurements of I_0 from the Orbit 2μ p-well process. At present we only have data from one Orbit run. We computed I_0 for a device on 12 chips and obtained an average value of 3.971e-17 and a standard deviation of 2.55e-17. (The within chip standard deviation was about 0.5 the between chip value.) Using the value $I_0 = 3.971\text{e-}17$ and $V_t = -.795$ we obtained the following results. Table 1 shows the basic measurements on a p-transistor for 12 die from a p-well MOSIS run. All die came from the same site on separate wafers.

Table 1: Measurements on a Test Transistor

Chip No.	—m—	kappa	Io	Id@0.55	Id@0.70	Vth
1	11.87	0.6832	9.614e-18	3.211e-11	1.939e-09	-0.8098
2	11.37	0.6545	7.186e-17	1.267e-10	6.394e-09	-0.7616
3	11.63	0.6695	1.918e-17	4.745e-11	2.632e-09	-0.7994
4	11.76	0.6772	8.545e-18	2.524e-11	1.467e-09	-0.814
5	11.54	0.6645	4.347e-17	9.606e-11	5.153e-09	-0.7678
6	11.53	0.6639	3.816e-17	8.35e-11	4.46e-09	-0.7728
7	11.55	0.6646	3.701e-17	8.231e-11	4.417e-09	-0.7737
8	11.44	0.6584	5.451e-17	1.056e-10	5.428e-09	-0.7687
9	11.68	0.6723	2.512e-17	6.604e-11	3.716e-09	-0.7799
10	11.73	0.675	1.535e-17	4.297e-11	2.463e-09	-0.7993
11	11.37	0.6548	7.443e-17	1.322e-10	6.688e-09	-0.7557
12	11.35	0.6534	7.927e-17	1.363e-10	6.845e-09	-0.7556
Mean	11.57	0.666	3.971e-17	8.137e-11	4.3e-09	-0.7799
Std dev	0.1689	0.009725	2.55e-17	3.92e-11	1.876e-09	0.02064

Using these data we computed the correlation bwttern $log(I_0)$, κ and V_t. The resulting correlation matrix is:

Table 2: Correlation of $log(I_0)$ V_t and κ

$log(I_0)$	V_t	κ
1.0000	0.9868	-0.9707
0.9868	1.0000	-0.9317
-0.9707	-0.9317	1.0000

From this information we computed regressions, using V_t as the independent variable. These are shown in Figures 10 and 11.

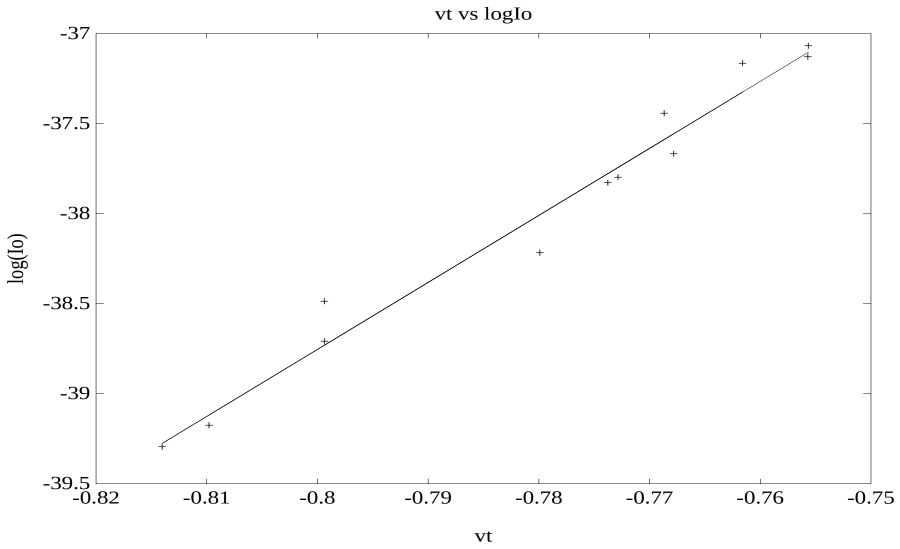

Figure 10: Dependence between V_t and I_0

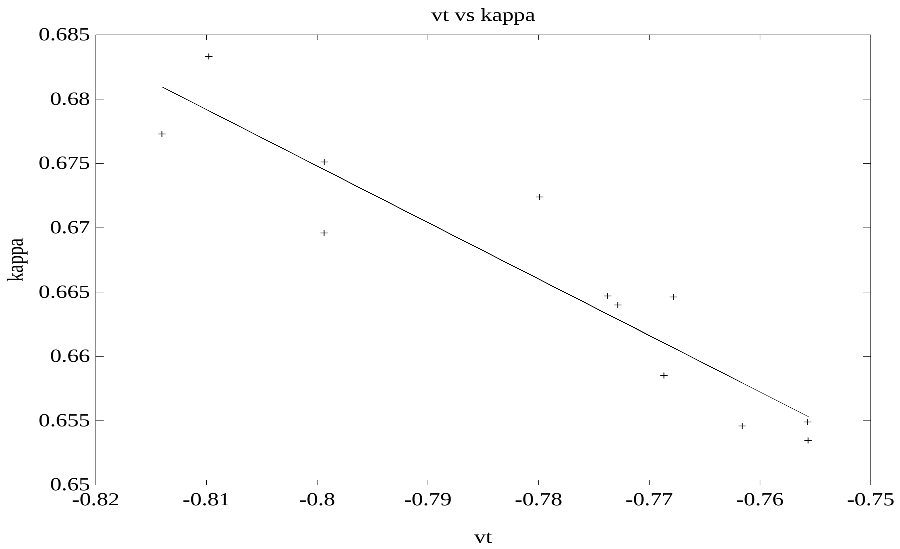

Figure 11: Dependence between V_t and κ

The regression equations for these two regressions are:

$$log(I_0) = -8.98 + 37.22V_t$$

and

$$\kappa = .32 - .44V_t$$

With this information it is possible to compute model paramters from measured values of V_t. One can consider three obvious choices of the source for values of V_t:

1. Values measured from each device, as in Table 1.
2. Value taken from the average V_t as from Table 1.

3. Value of V_t taken from process batch measurements as reported by MOSIS.

Preliminary analysis has been carried out to investigate the effects on model accuracy of prediction using these three sources for V_t. The three following Figures show an example result from the 12 measurements shown in Table 1.

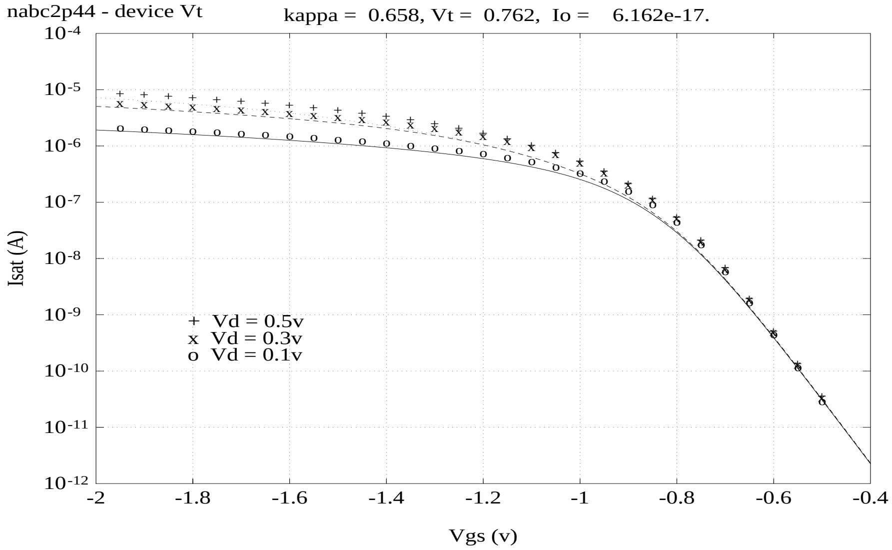

Figure 12: Model Approximation using Device V_t

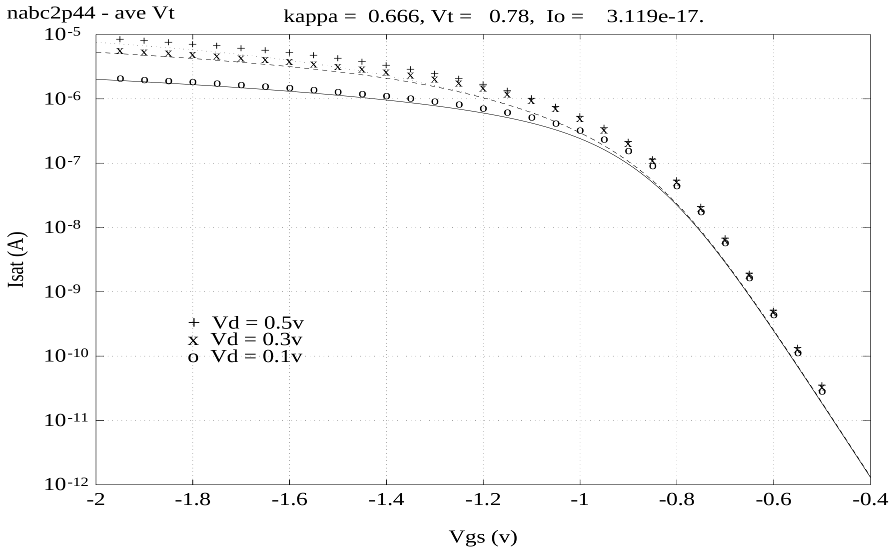

Figure 13: Model Approximation using Average V_t

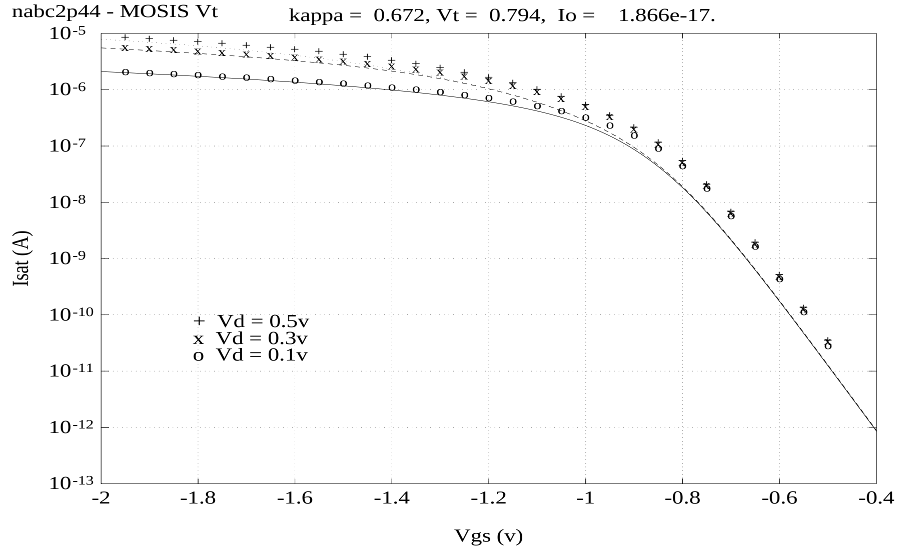

Figure 14: Model Approximation using MOSIS V_t

7.2 Possible generalizations of the EVO Model

It is not clear that the EVO model, in its present form, produces the best possible results. In particular, for shorter channel lengths (which will find increasing use as λ is reduced) it will begin to make sense to consider a model that goes to behavior closer to linear since velocity saturation in the channel comes into effect quickly for short channel devices. Thoughts in this direction suggest a form:

$$f(x) = \ln^a(d + e^{bx-c})$$

Choice of a, b, c, and d would permit modification of the rate of the transition from exponential behavior to behavior of the form x^a.

As we acquire more data and experience with use of the model we will consider exploration of some aspects of this generalization.

8. Conclusion

The main conclusion of this paper is that subthreshold device behavior can be modelled and predicted with reasonable accuracy. However, care is required to obtain device parameter measurements that are appropriate to subthreshold operation. In particular, the measurement and use of V_t requires special attention.

As channel lengths become shorter, accurate modelling will be made even more difficult for two reasons. Velocity saturation will tend to cause the classical square-law model to be inaccurate, with behavior tending toward linear. And, the size of the transition region between sub and above-threshold will become an increasing proportion of the operating range of devices.

Acknowledgements

I first learned about the Enz/Vittoz approximation as part of using the analog simulator called anaLOG. This design tool was provided by Carver Mead's Group at Caltech. Essential help in understanding anaLOG and the EVO model was provided by John Lazzaro, now at the University of California at Berkeley. Neal Bhadkamkar carried out the time-consuming measurements on the transistors as reported in Section 7.1. Conversations with and new data from Andreas Andreou at Johns Hopkins helped to focus my attention on actual sources of variation. My general interest in exploring the effectiveness of subthreshold analog computation is inspired by Carver Mead, as expressed in [3] and elsewhere.

References

[1] C.C. Enz, "High Precision CMOS Micropower Amplifiers," Thesis No 802 (1989), Ecole Polytechnique Federale de Lausanne.

[2] E.A. Vittoz, "Micropower Techniques," in *Design of MOS VLSI Circuits for Telecommunications,* eds. Tsividis, Y. and Antognetti, P., Prentice-Hall, 1985, pp. 104-144.

[3] C.A. Mead, *Analog VLSI and Neural Systems,* Addison-Wesley, 1989.

[4] M.A. Maher and C.A. Mead, "A Physical Charge-Controlled Model for MOS Transistors," in *Advanced Research in VLSI,* ed. P. Losleben, MIT Press, 1987, pp.211-229.

[5] R. M. Swanson, "Complementary MOS Transistors in Micropower Circuits," Ph.D. Thesis, Stanford University, Stanford, CA., 1974.

[6] Y. Tsividis and G. Masetti,"Problems in Precision Modelling of the MOS Transistor for Analog Applications," *IEEE Transactions on Computer-Aided Design,* CAD-3, 1984. pp. 72-79.

[7] A. Pavasović, A. G. Andreou, and C. R. Westgate, "Characterization of CMOS Process Variations by Measuring Subthreshold Current," *Nondestructive Characterization of Materials IV,* eds. R. E. Green and C. O. Ruud, Plenum Press, 1991, pp.xx-yy.

[8] A. Pavasović, "Subthreshold Region MOSFET Mismatch Analysis and Modelling for Analog VLSI Systems," Ph.D. Dissertation, The Johns Hopkins University, 1990.

[9] V. K. De and J. D. Meindl, "Three-Region Analytical Models for MESFET's in Low-Voltage Digital Circuits, *IEEE J. of Solid-State Circ.*, vol. 26, No. 6, June 1991.

Appendix: MatLab Listing

```
function [Ids] = jlvit(Vg, Vs, Vd, W, L, beta, kappa, Vt, Io)
% function [Ids] = jlvit(Vg, Vs, Vd, W, L, beta, kappa, Vt, Io)
%
% Computes MOS transistor behavior using a simplified (by John
% Lazzaro) Vittoz model.  It should work fairly well for sub and
% above threshold.
% W, L, beta, kappa, and Vt are design and technology parameters:
% Some typical values are:
%   W =     6um
%   L =     6um   The model only really uses W/L
%   beta =  u*Cox*(W/L) (from Vittoz) = 50 uA/V^2 (MOSIS VTI 2u CMOS)
%   kappa (1/n in Vittoz notation) = 0.7v (Carver)
%   Vt =    0.9v (Carver and MOSIS)
%
% Internal parameters:
%   Vk = kT/q = 25mv at room temp.
%   Io = the unexplained part of the "great big" preexponential
%        constant (See Carver)
%        Value of 16.4 needed to fit Carver's curves in Figs 3.6
%             and 3.7 and recent typical MOSIS fabricated devices.
%
% Result:  Ids in A.
%
Vk = .025;
k1 = 10^(-6)*Io*2*(W/L)*beta*Vk^2/kappa;
If = (log(1 + exp((1/(2*Vk))*(kappa*(Vg - Vt) - Vs)))).^2;
Ir = (log(1 + exp((1/(2*Vk))*(kappa*(Vg - Vt) - Vd)))).^2;
Ids = If - Ir;
Ids = k1*Ids.*(1 + 0.05*Vd);
```